

## Nonlinear finite element modeling of FRP-wrapped UHPC columns

Soner Guler\*, Alperen Çopur and Metin Aydoğan

*Faculty of Civil Engineering, Istanbul Technical University, 34469, Istanbul, Turkey*

*(Received October 24, 2012, Revised April 8, 2013, Accepted May 11, 2013)*

**Abstract.** The primary aim of this study is to develop a three dimensional finite element (FE) model to predict the axial stress-strain relationship and ultimate strength of the FRP-wrapped UHPC columns by comparing experimental results. The reliability of four selected confinement models and three design codes such as ACI-440, CSA-S806-02, and ISIS CANADA is also evaluated in terms of agreement with the experimental results. Totally 6 unconfined and 36 different types of the FRP-wrapped UHPC columns are tested under monotonic axial compression. The values of ultimate strengths of FRP-wrapped UHPC columns obtained from the experimental results are compared and verified with finite element (FE) analysis results and the design codes mentioned above. The concrete damage plasticity model (CDPM) in Abaqus is utilized to represent the confined behavior of the UHPC. The results indicate that agreement between the test results and the non-linear FE analysis results is highly satisfactory. The CSA-S806-02 design code is considered more reliable than the ACI-440 and the ISIS CANADA design codes to calculate the ultimate strength of the FRP-wrapped UHPC columns. None of the selected confinement models that are developed for FRP-wrapped low and normal strength concrete columns can safely predict the ultimate strength of FRP-wrapped UHPC columns.

**Keywords:** ultra-high performance concrete; fiber reinforced polymer; finite element analysis; ultimate strength; design codes

---

### 1. Introduction

For many years, structural engineers have used different methods and techniques to retrofit existing structures by providing external confining stresses. Jacketing is the most commonly used method for strengthening of columns. The most popular types of jacketing are steel jacket, reinforced concrete jacket and fiber reinforced polymer (FRP) composite jacket. Steel jacketing is an effective technique to enhance the seismic performance of columns. The steel jacket is manufactured in two shell pieces and welded in the field around the column. However, this method requires difficult welding work and, in a long term, the potential problem of corrosion remains unsolved. Reinforced concrete jacketing of the columns consists of added concrete with

---

\*Corresponding author, Ph.D., E-mail: mmh356@yahoo.com

<sup>a</sup>Professor

<sup>b</sup>Senior Lecturer

longitudinal and transverse reinforcement around the existing columns. While this type of strengthening enhances the axial strength, shear strength, and flexural strength of the column, it is not sufficiently successful for improving the ductility of the columns (Al-Salloum 2007, Waghmare 2011). In recent years, intensive attention is concentrated on the use of fiber-reinforced polymer (FRP) composite materials for structural rehabilitation and strengthening. FRP composite materials are becoming more frequently used in civil engineering structures. The principal advantages of this technique are the high strength-to-weight ratio, good fatigue properties, non-corroding characteristics of the fiber reinforced polymers (FRP), and the facility of its application. The maximum efficiency of confining systems using FRP materials is reached in case of columns with circular cross-section and is explained by the fact that the entire section of the column is involved into the confinement effect (Cozmanciuc *et al.* 2009).

Many studies (Fardis and Khalili 1982, Samaan *et al.* 1997, Saafi *et al.* 1999, Shahawy *et al.* 2000, Shehata *et al.* 2002, Lam and Teng 2003, Spoelstra and Monti 1999, Wang and Wu 2008, Hu and Wang 2009, Elwan and Rashed 2011, Pimanmas and Xuan 2011) report that the strength and ductility of axially loaded concrete columns can be significantly increased using FRP-jacketing system. Most of these studies are based on small-scale normal strength concrete columns. In parallel with these studies, very few tests are performed by researchers to investigate the behavior of FRP-wrapped high- and ultra-high strength concrete columns (Harmon and Slattery 1992, Mandal *et al.* 2005 and Zohrevand *et al.* 2011). In addition to these studies, non-linear finite element models are thoroughly studied by many researchers to simulate the axial behavior of FRP-wrapped low and normal strength concrete columns. The axial behavior of FRP-wrapped concrete columns with different type of wrapping materials is examined by Lau and Zhou (2001) using the FE method. The results show that the ultimate strength of the FRP-wrapped concrete columns is governed by mechanical properties such as elastic modulus and Poisson's ratio of the FRP sheet. Rochette and Labossiere (2000) investigate that the influence of wrap thickness and cross-section type on concrete columns strengths. In addition, they utilize an incremental FE technique, based on (Drucker and Prager 1952) failure criteria, to evaluate the response of FRP-wrapped concrete columns. A non-linear finite element model is developed by Mirmiran *et al.* (2000) for FRP-wrapped concrete columns using non-associative Drucker-Prager plasticity model. The results clearly show that Drucker-Prager plasticity effectively estimates the axial stress-strain relationship of the FRP-wrapped concrete columns. Doran *et al.* (2009) develop a non-linear FE model of axially loaded FRP-wrapped square and rectangular concrete columns. Confining stresses obtained from non-linear FE analysis are compared with uniform confining pressures for cylindrical specimens. The results signify that lateral confinement stress may be considered much less effective on flat sides in comparison with corner sides. Therefore, they emphasize that this effect can be taken into account in FE modeling of FRP-wrapped square and rectangular concrete columns.

### 1.1 Objective

Nowadays ultra-high strength concretes such as UHPC with compressive strengths up to 200 MPa can be produced easily with regard to developments in concrete technology. This can be achieved by a reduction of the water/binder ratio and an increase of the packing density by aggregate and admixture optimization. Moreover, the high density of UHPC enables a considerably higher resistance against carbonation, chloride penetration, freeze-thaw loading in comparison to low and normal strength concretes. Thus, due to its outstanding characteristics, the

use of UHPC especially in bridge columns that is needed high durability requirements is becoming more and more popular. Although there are many experimental and numerical studies on FRP-wrapped low and normal strength concrete columns, there are relatively little research on FRP-wrapped UHPC columns. Up to present, a reliable FE model is not developed by the researchers to simulate the axial behavior of FRP-wrapped UHPC columns. In addition to this, the knowledge on the reliability and the applicability of the confinement models and the design codes to predict the ultimate strength of the FRP-wrapped UHPC columns is still limited. Thus, this study is carried out to fill this gap in the literature.

The first aim of this study is to develop a FE model to predict the axial stress-strain curves and ultimate strength of the FRP-wrapped UHPC columns. For this purpose, three dimensional nonlinear FE model is established and verified by comparing to experimental results. The commercial FE program Abaqus is employed to examine the numerical simulation of the FRP-wrapped UHPC columns. Secondly, the reliability of the three design codes that is most commonly used in America and Canada countries is examined for the FRP-wrapped UHPC columns. Finally, the applicability of the selected four confinement models that are developed for FRP-wrapped low and normal strength concrete columns is also evaluated for the FRP-wrapped UHPC columns.

## 2. Experimental program

### 2.1 Specimen layout

Totally 6 unconfined and 36 different types of FRP-wrapped UHPC columns are tested under monotonic axial compression in the Structural and Earthquake laboratory of the Istanbul Technical University (ITU). This research program is supported by scientific research project BAP-ITU and Istanbul Concrete Production Corporation (ISTON). The UHPC used in this study is produced by ISTON that is well known throughout the region for high quality concrete productions. The plastic pipes with length of 200 mm and diameter of 100 mm are cut and prepared for the casting of concrete in the structural laboratory of ISTON. The UHPC is produced and cast into the plastic pipes. The specimens are kept in the moulds for 24 h at room temperature of 20°C. After demolding, the specimens are exposed to steam curing at 90°C for 4 days. Heating rate of steam cure treatment is 11°C/h. After completion of their curing periods, the specimens are kept in laboratory atmosphere for cooling, and then cleaned and prepared for the wrapping. The epoxy resin MGS-L285 and hardener are used for bonding the FRP jackets on the concrete columns. The specimens are wrapped by FRP jackets (2, 3, 4, and 5 plies) in transverse direction with 0-degree orientation. The last FRP layer is wrapped around the cylinder with an overlap of the diameter of the column to prevent sliding or debonding of the FRP sheets during tests. Carbon, Glass and Aramid fiber sheets are cut and impregnated with epoxy resin by the hand lay-up technique. The top and bottom surfaces of all the columns are grinded smooth for the compression tests. Then, the wrapped concrete columns are left at room temperature for one week for the epoxy to harden sufficiently before testing. Test data, geometrical and mechanical properties of the specimens are given in Tables 1 and 2, respectively.

A batch of UHPC is produced by using very fine sand, cement, silica fume, super plasticizers and steel fibers. Cylindrical 100 × 200 mm samples are prepared in accordance to Turkish Standard (TS EN 206 2002) and (TS EN 12390 2002) to determine the compressive strength of the concrete. The 28-day average compressive strength of the concrete cylinders is 159 MPa.

Table 1 Test data and specimen properties

Specimen group	Ultimate Strength (MPa)	Ultimate Strain	Number of identical specimens	Core diameter (mm)	Height (mm)	Number of FRP layers	Thickness of FRP (mm)
P	159.00	0.0109	6	100	200	N/A	N/A
C2	168.79	0.0127	3	100	200	2	0.70
C3	185.51	0.0143	3			3	1.05
C4	199.47	0.0174	3			4	1.40
C5	235.04	0.0202	3			5	1.75
G2	162.89	0.0133	3	100	200	2	0.70
G3	164.04	0.0158	3			3	1.05
G4	179.19	0.0206	3			4	1.40
G5	185.72	0.0244	3			5	1.75
A2	164.76	0.0127	3	100	200	2	0.64
A3	177.83	0.0139	3			3	0.96
A4	185.00	0.0178	3			4	1.28
A5	195.06	0.0211	3			5	1.60

Table 2 Geometrical and mechanical properties of FRP sheets as reported by the manufacturer

	CFRP	GFRP	AFRP	Epoxy resin (L285)	CFRP fibers with epoxy	GFRP fibers with epoxy	AFRP fibers with epoxy
Tensile Strength (MPa)	3950	2790	2926	70-80	910	770	820
Tensile modulus (GPa)	238	82.7	110	3-3.3	51	30	38
Ultimate Elongation (%)	1.7	3.2	2.5	5-6.5			
Density (g/cm <sup>3</sup> )	1.76	2.6	1.44	1.18-1.20			
Thickness (mm)	0.35	0.35	0.32	-			
Weight per unit area (g/m <sup>2</sup> )	245	280	170	-			

Table 3 UHPC mix proportion

	Mix Proportions (kg) for 1m <sup>3</sup> concrete
Cement	1000
Siliceous sand(0.5-1.5 mm)	251
Siliceous powder (0-0.5 mm)	377
Silica fume	250
Super plasticizer	31.75
Water	230
Steel fiber	500
Total	2640

The regular CEM I PÇ 42.5R is used as cement material in the mix. Two different steel fibres, OL 6/16 and Dramix ZP 305, are added into the mix. The fibers in the mix with a diameter of 0.55 mm, a length of 30 mm, and tensile strength of 1100 MPa. The short ones, OL 6/16, are straight

fibers without hooked ends as meso fibers, 6 mm in length and 0.16 mm in diameter. The tensile strength of OL 6/16 steel fibers is 2250 MPa. Water-binder (cement + silica fume) ratio is kept constant at 0.18. The typical mix composition of the UHPC used in this study is given in Table 3.

### 3. Finite element model

#### 3.1 Finite element types and mesh

Three-dimensional composite solid element C3D8R is used to model the concrete core. This element is an 8-noded solid brick element with three translation degrees of freedom per node ( $x$ ,  $y$ , and  $z$  directions). This element has capability of both cracking in tension and crushing in compression. It is also capable of plastic deformation and creep. The FRP wrap is modeled by 4-noded linear elastic S4R shell element. S4R shell element is a 3-D element having membrane (in-plane) stiffness but, no bending (out-of plane) stiffness. The element has three-degrees of freedom at each node: translations in the nodal  $x$ ,  $y$ , and  $z$  directions. The element has variable thickness, stress stiffening, large deflection, and a cloth option. Cloth option is used for a tension-only behavior. This non-linear option acts like a cloth in that tension loads will be supported but, compression loads will cause the element to wrinkle (Abaqus User's Manual version 6.8 2008). The 8-node C3D8R solid element and the 4-node S4R shell element are shown in Fig. 2, respectively.

The mesh size is determined to be 1 mm in each direction. Fig. 3 shows the finite element mesh of a CFRP-wrapped UHPC column with 2 plies of FRP, 100 mm outer diameter and 200 mm length. Due to symmetry, only a quarter of the column is modeled, as shown in Fig. 3. End of the columns is fixed where there is no degree of freedom. A perfect bond between the concrete and FRP sheets are assumed due to two-component resin epoxy provide a strong interaction between these two materials.

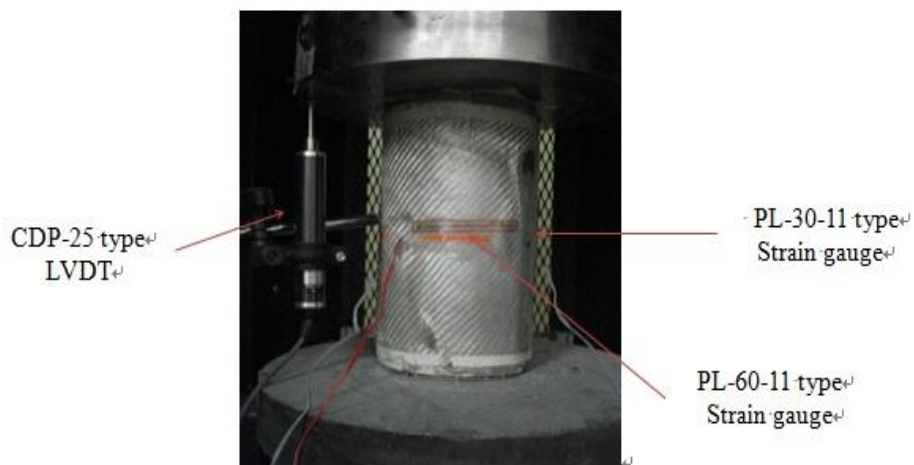


Fig. 1 Test setup

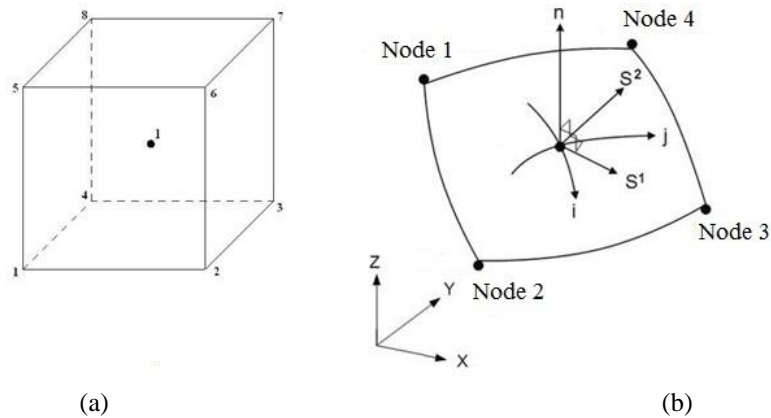


Fig. 2 (a) 8-node C3D8R solid element (b) 4-node S4R shell element

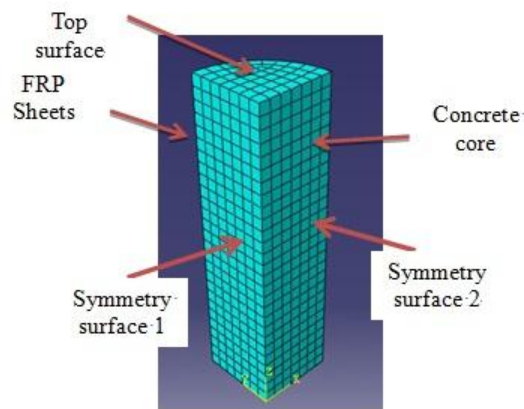


Fig. 3 Element mesh of FE model for FRP-wrapped UHPC column

### 3.2 Material modeling of confined concrete

The Concrete Damage Plasticity Model (CDPM) is briefly presented in the next section. The CDPM in Abaqus uses approach of isotropic damage in combination with isotropic tensile and compressive plasticity to exhibit the inelastic behavior of concrete core. In the model, Poisson's ratio of concrete ( $\nu_c$ ) and tangent elastic modulus of concrete ( $E_c$ ) is taken as 0.2 and 24 GPa, respectively. Typical stress-strain curves obtained from concrete cylinders loaded in uniaxial compressive tests are utilized in the FE model.

#### 3.2.1 Yield criterion

Abaqus plastic-damage concrete model (CDPM) is utilized for modeling inelastic behavior of concrete. The yield criterion proposed by Lubliner *et al.* (1989) and further developed by Lee and Fenves (1998) is adopted in the FE model. In the original formulation, the yield surface (F) is an

extended version of Drucker-Prager type yield criterion and formulated in terms of effective stresses given below Eq. (1)-(9).

$$F(\bar{\sigma}, \bar{\varepsilon}^{pl}) = \frac{1}{1-\alpha} \left( \bar{q} - 3\alpha\bar{p} + \beta(\bar{\varepsilon}^{pl})(\hat{\sigma}_{max}) - \gamma(-\hat{\sigma}_{max}) - \bar{\sigma}_c \left( \bar{\varepsilon}_c^{pl} \right) \right) \quad (1)$$

$$\bar{p} = -\frac{1}{3}\bar{\sigma}:I \quad (2)$$

$$\bar{q} = \sqrt{\frac{3}{2}\bar{S}:\bar{S}} \quad (3)$$

$$\bar{S} = \bar{p}I + \bar{\sigma} \quad (4)$$

$$\bar{\sigma} = D^{el}:(\epsilon_{total} - \epsilon^{pl}) \quad (5)$$

$$\beta(\bar{\varepsilon}^{pl}) = \frac{\bar{\sigma}_c(\bar{\varepsilon}_c^{pl})}{\bar{\sigma}_t(\bar{\varepsilon}_t^{pl})} (1 - \alpha)(1 + \alpha) \quad (6)$$

$$\alpha = \frac{\sigma_{bo} - \sigma_{co}}{2\sigma_{bo} - \sigma_{co}} \quad (7)$$

$$\gamma = \frac{3(1-K_c)}{2K_c - 1} \quad (8)$$

$$K_c = \frac{\bar{q}(TM)}{\bar{q}(CM)} \quad (9)$$

where  $\bar{p}$  is the effective hydrostatic pressure,  $\bar{q}$  is the *von Mises* equivalent effective stress,  $\bar{\sigma}$  is the effective stress,  $D^{el}$  is the initial (undamaged) elasticity matrix,  $\epsilon_{total}$  is the total strain,  $\epsilon^{pl}$  is the plastic strain,  $\bar{\varepsilon}^{pl}$  is the effective plastic strain,  $\beta(\bar{\varepsilon}^{pl})$  is the coefficient of the Drucker-Prager yield function,  $\bar{S}$  is the deviatoric part of the effective stress ( $\bar{\sigma}$ ),  $\hat{\sigma}_{max}$  is the maximum principal effective stress,  $\alpha$  and  $\gamma$  are the dimensionless material constants of the Drucker-Prager yield function,  $\bar{\sigma}_c(\bar{\varepsilon}_c^{pl})$  and  $\bar{\sigma}_t(\bar{\varepsilon}_t^{pl})$  are the effective compressive and tensile cohesion stresses.

In the biaxial compression, the constants  $\alpha$  and  $\gamma$  are determined from the initial equibiaxial and uniaxial compressive yield stresses  $\sigma_{bo}$  and  $\sigma_{co}$ .  $\frac{\sigma_{bo}}{\sigma_{co}}$  is the ratio of initial equibiaxial compressive yield stress to initial uniaxial compressive yield stress which was assumed to be 1.16 in this study. The ratio of second stress invariant on the tensile meridian,  $\bar{q}(TM)$ , to that on the compressive meridian,  $\bar{q}(CM)$  is notated by  $K_c$  and is taken as 0.67.

Table 4 Damage parameters in CDPM for the UHPC

$\varphi$	$f_{bo}/f_{co}$	$K_c$	$e$
18	1,16	0,67	0,01

### 3.2.2 Flow rule

The plastic-damage model assumes non-associated potential flow with the following flow potential function ( $G$ )

$$G = -\bar{p}\tan\varphi + \sqrt{(e\sigma_{t0}\tan\varphi)^2 + \bar{q}^2} \quad (10)$$

$\varphi$  is the dilation angle measured in the  $p - q$  plane at high confining pressure, and is taken as 18.  $\sigma_{t0}$  is the uniaxial tensile stress at failure, and  $e$  is a parameter, referred to as a eccentricity, that defines the rate at which the function approaches the asymptote (the flow potential tends to a straight line as the eccentricity tends to zero). In this study, a value of 0.01 is assumed for the eccentricity.

As a result of a large number of FE analysis to accurately simulate the axial behavior of FRP-wrapped UHPC columns, the parameters that are required for the concrete damage plasticity model (CDPM) in Abaqus are obtained and collectively presented in Table 4.

Here,  $\varphi$  is the dilation angle,  $f_{bo}/f_{co}$  is the ratio of the biaxial compressive strength to the uniaxial compressive strength of the concrete,  $K$  is the ratio of the second stress invariant on the tensile meridian, to that on the compressive meridian.  $e$  is an eccentricity of the plastic potential surface.

## 4. Design codes

### 4.1 ACI-440

The design code of ACI-440 provides design equations for axially loaded FRP-wrapped short circular columns. The gain in concrete strength mainly depends on the passive confinement exerted by the FRP sheets. The FRP sheets in the axial direction of the column are not considered to provide any increase in the axial load carrying capacity. The ultimate strength of the FRP-wrapped concrete columns according to the Committee ACI-440 can be given below in Eqs. (11) and (12).

$$f_{cc} = f_c \left[ 2.25 \sqrt{1 + 7.9 \frac{f_l}{f_c}} - 2 \frac{f_l}{f_c} - 1.25 \right] \quad (11)$$

$$f_l = \frac{k_a \rho_f f_{fe}}{2} \quad (12)$$

Here;  $f_c$  is the unconfined compressive strength;  $f_l$  is the lateral confinement pressure;  $k_a$  is the efficiency coefficient (for circular columns  $k_a = 1$ );  $\rho_f$  is the confining FRP volumetric ratio evaluated by  $4nt_f/d$ ;  $n$  is the number of FRP layers;  $t_f$  is the thickness of one FRP layer;  $d$  is the diameter of circular column;  $f_{fe}$  is the FRP tension strength evaluated by  $\varepsilon_{fe}E_f$ ;  $E_f$  is the modulus of elasticity of FRP; and  $\varepsilon_{fe}$  is the effective strain of FRP.

#### 4.2 CSA-S806-02

According to the Canadian Standards Association S806-02 the ultimate strength “ $f_{cc}$ ” can be evaluated by Eq. (13)-(15).

$$f_{cc} = 0.85f_c + k_1k_c f_l \quad (13)$$

$$f_l = \frac{2t_j f_{Fj}}{D} \quad (14)$$

$$k_1 = 6.7(k_c f_l)^{-0.17} \quad (15)$$

Here;  $f_l$  is the lateral confinement pressure;  $t_j$  is the thickness of FRP jacket;  $D$  is the diameter of circular column;  $f_{Fj}$  is the stress in FRP jacket; and  $k_c$  is the confinement coefficient (for circular columns  $k_c = 1$ ).

#### 4.3 ISIS CANADA

The ultimate strength according to Intelligent Sensing for Innovative Structures Canada Network of Centers of Excellence can be obtained by given formulas below

$$f_{cc} = f_c(1 + \alpha_{pc} w_w) \quad (16)$$

$$w_w = \frac{2f_{IFRP}}{\phi_c f_c} \quad (17)$$

$$f_{IFRP} = \frac{2N_b \phi_{FRP} f_{FRPu} t_{FRP}}{D} \quad (18)$$

Here;  $\alpha_{pc}$  is the performance coefficient (taken as 1 for circular columns);  $w_w$  is the volumetric strain ratio;  $f_{IFRP}$  is the lateral confinement pressure;  $N_b$  is the number of FRP layers;  $t_{FRP}$  is the thickness of one FRP layer;  $f_{FRPu}$  is the ultimate tensile strength of FRP;  $\phi_{FRP}$  is the resistance reduction factor of FRP; and  $D$  is the diameter of circular column.

To provide a certain amount of ductility and thus ensure an effective confinement, the ISIS guidelines require a minimum confining pressure equal to 4 Mpa, that is

$$f_{IFRP} \geq 4MPa \quad (19)$$

Additionally, a maximum confining pressure is defined to limit the axial compressive strains, that is

$$f_{IFRP} \leq \frac{0.29 f_c}{\alpha_{pc}} \quad (20)$$

#### 4.4 Results and discussions

##### 4.4.1 Axial stress-strain curves

The axial stress-axial strain curves of the all types of FRP-wrapped UHPC columns are obtained and compared with the FE analysis results. Figs. 4, 5 and 6 show the average axial stress-axial strain curves for GFRP, AFRP, and CFRP- wrapped UHPC columns, respectively.

The stress-strain curves of all the types of FRP-wrapped UHPC columns show a typical bilinear trend with strain hardening. Generally, three zones are observed for the stress-strain curves of the FRP-wrapped UHPC columns. The first zone is mainly a linear response controlled by the stiffness of the unconfined UHPC columns. No confinement effect provided by the FRP-wraps is launched at this stage due to lateral strains are very small. In the second zone, a non-linear transition occurs as the UHPC has a tendency to dilate or to expand that causing an interaction between the FRP sheets and the UHPC. Finally, in the third zone, the multiple distributed cracks of the UHPC significantly increase and the FRP-confinement is fully activated; the response is mainly dependent on the stiffness and confinement ratio of the FRP material.

The values of ultimate strengths obtained from the test results ( $f_{cc,exp}$ ), the FE analysis ( $f_{cc,FE}$ ), and the design codes ( $f_{cc,ACI}$ ;  $f_{cc,CSA}$ ; and  $f_{cc,ISIS}$ ) are given in Table 3. As seen in Figs. 4, 5 and 6, the entire bilinear curve of the FRP-wrapped UHPC columns can be successfully predicted by the FE model. The biggest difference of ultimate strength between experimental and the FE analysis results is 16% for the AFRP-wrapped UHPC columns with 5 number of FRP sheets. The values of ultimate strength obtained from the FE model are little higher than those with the experimental results. However, the predictions of the FE model are in much closer agreements for the FRP-wrapped UHPC columns with smaller confinement ratio (2 and 3 layers of FRP sheets) than those with greater confinement ratio (4 and 5 layers of FRP sheets).

##### 4.4.2 Failure modes

A typical failure mode is observed for all the columns. Before failure, cracking noises are frequently heard. Location of failure is not limited to a small region located at the mid-height of the columns. The failure of the FRP sheets is initiated away from the overlap region at mid-height of the specimen and propagated to the top and bottom surfaces of the specimens. The CFRP and AFRP-wrapped UHPC columns fails in a sudden and explosive manner while the GFRP -wrapped UHPC columns is more gradual and less explosive manner. The CFRP and AFRP- wrapped UHPC columns exhibit more brittle behavior compared with the GFRP-wrapped UHPC columns after the first peak load. For all the FRP-wrapped UHPC columns, delamination is not observed at the overlap region of the FRP sheets which verify the adequate stress transfer over the splice. The failure modes of the FRP-wrapped UHPC columns obtained from the test results and FE analysis is illustrated in Figs. 7 and 8, respectively. As shown in Fig. 8, the stress values at the ultimate condition are concentrated on the mid-height of the columns. These values are decreasing towards top and bottom surfaces of the columns.

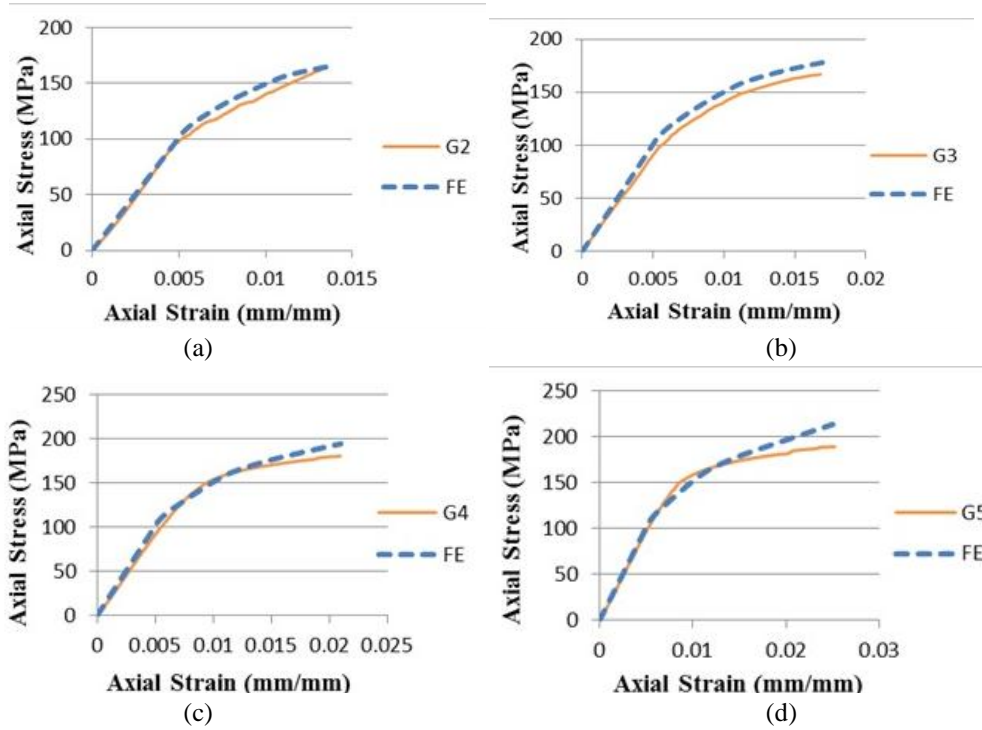


Fig. 4(a)-(d) Comparison of average axial stress-strain relationship of GFRP wrapped UHPC columns

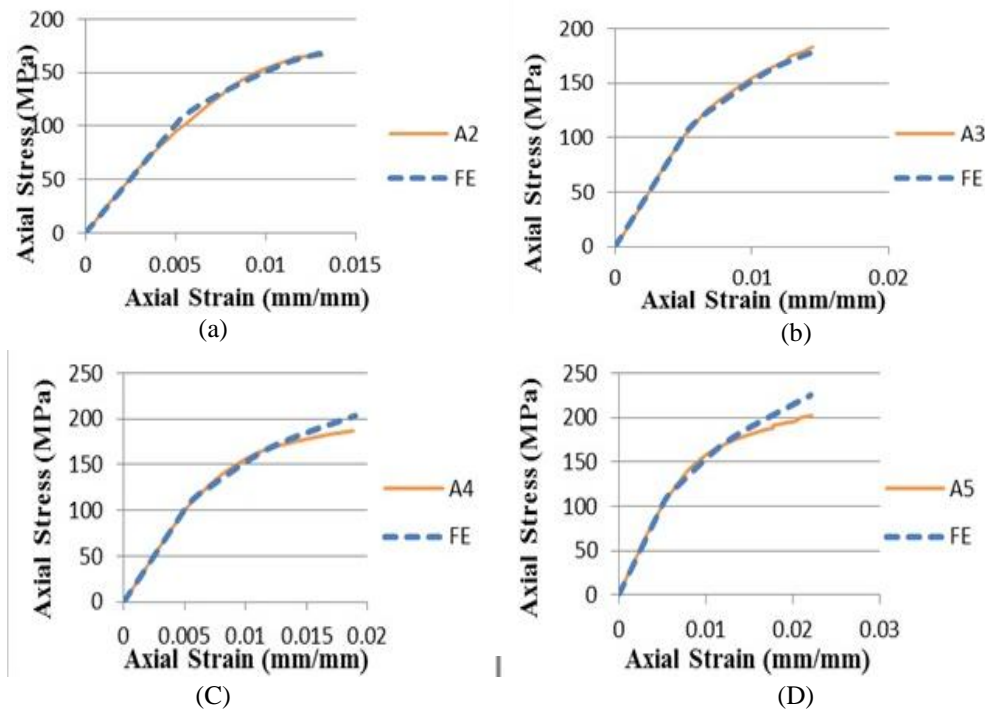


Fig. 5(a)-(d) Comparison of average axial stress-strain relationship of AFRP wrapped UHPC columns

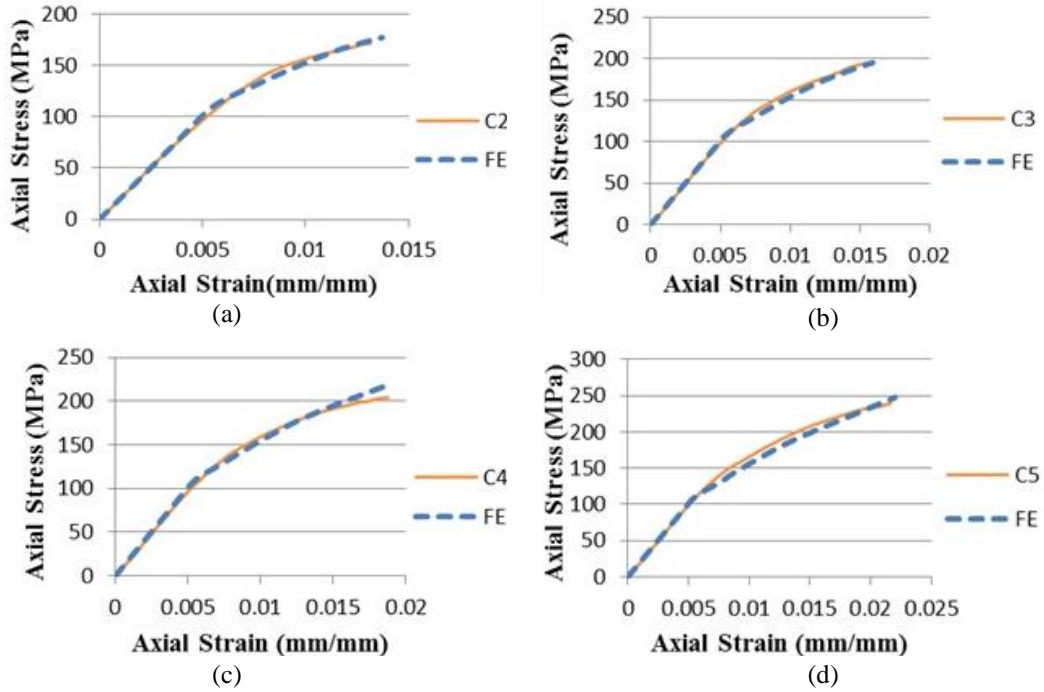


Fig. 6(a)-(d) Comparison of average axial stress-strain relationship of CFRP wrapped UHPC columns

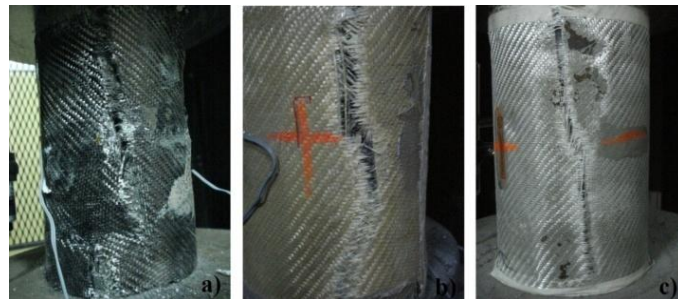


Fig. 7 Failure modes of the FRP-wrapped UHPC columns obtained from the test results (a) GFRP; (b) AFRP ; (c) CFRP

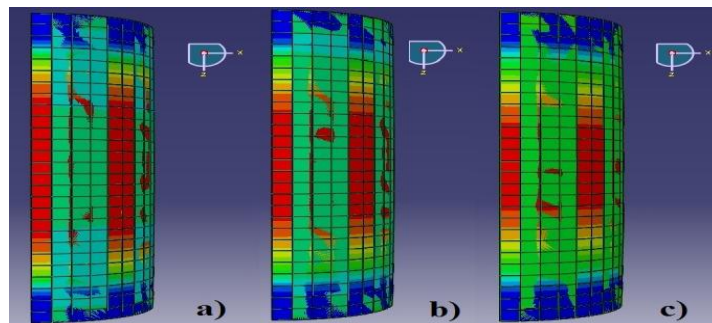


Fig. 8 Failure modes of the FRP-wrapped UHPC columns obtained from the FE analysis results (a); CFRP ; (b) AFRP ; (c) GFRP

4.4.3 Evaluation of design codes

According to the three design codes, the ultimate strengths mainly depend on the lateral confining pressure exerted by the FRP sheets. The ISIS design code enforces a maximum confining pressure equal to  $0.29f_c'$  and a minimum lateral confining pressure equal to 4 MPa. Furthermore, to calculate the ultimate strength, the ISIS design code also takes into account the FRP tensile strength, while the ACI-440 design code are independent of the FRP tensile strength and, especially, are based on limiting the FRP strain. Similar to the ACI-440 design code, the CSA design code are based on limiting strain or the tensile strength of the FRP jacket. In addition, as seen in Eq. (13), the CSA design code requires a minimum confining pressure by applying a reduction coefficient of 0.85 to the unconfined concrete. This reduction coefficient provides a minimum limit and also diminishes the contribution of the FRP confinement to the concrete core. For this reasons, as seen in Fig. 11, the predictions of the CSA design code are more reasonable and more conservative than the ACI-440 and the ISIS design codes.

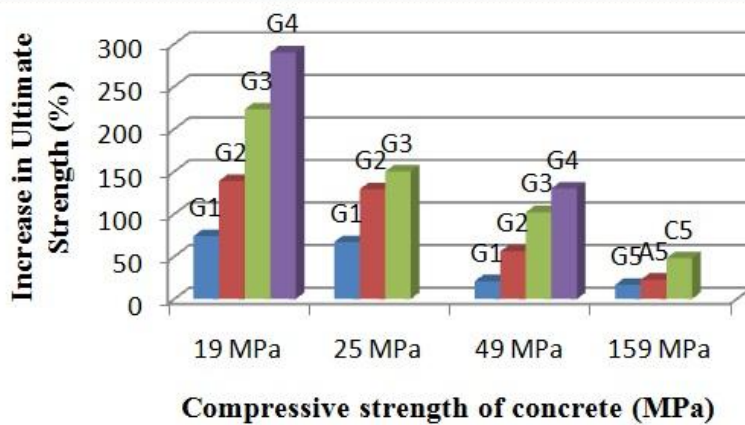


Fig. 9 The increase in ultimate strength for different range of concrete strength

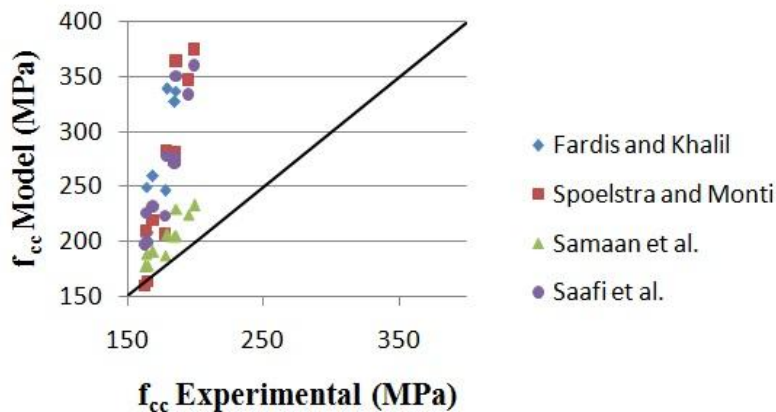


Fig. 10 Comparison of the confinement models with the experimental results

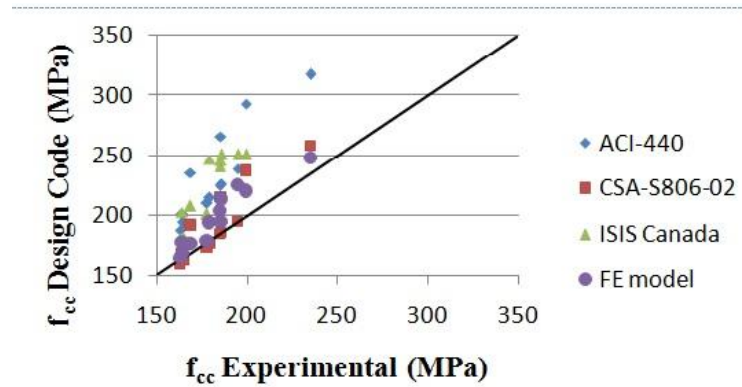


Fig. 11 Comparison of the design codes and the FE model with the experimental results

Table 5 Comparisons of numerical results, confinement models, and design codes with experimental results

Specimen	$f_{cc,exp}$ (MPa)	$f_{cc,FE}$ (MPa)	$\frac{f_{cc,FE}}{f_{cc,exp}}$	$\frac{f_{cc,Fardis}}{f_{cc,exp}}$	$\frac{f_{cc,Spoelstra}}{f_{cc,exp}}$	$\frac{f_{cc,Samaan}}{f_{cc,exp}}$	$\frac{f_{cc,Saafi}}{f_{cc,exp}}$	$\frac{f_{cc,ACI}}{f_{cc,exp}}$	$\frac{f_{cc,CSA}}{f_{cc,exp}}$	$\frac{f_{cc,ISIS}}{f_{cc,exp}}$
G2	162.89	165.09	1.01	1.26	0.98	1.09	1.21	1.16	0.97	1.11
G3	164.04	178.03	1.09	1.52	1.28	1.15	1.37	1.23	1.03	1.24
G4	179.19	194.20	1.08	1.89	1.57	1.15	1.55	1.20	0.99	1.38
G5	185.72	213.36	1.15	2.57	1.96	1.24	1.88	1.22	1.00	1.35
Av.			1.08	1.81	1.45	1.16	1.50	1.20	1.00	1.27
St.Dev.			0.05	0.49	0.36	0.05	0.25	0.03	0.02	0.10
A2	164.76	168.82	1.03	1.26	0.99	1.08	1.21	1.18	0.99	1.11
A3	177.83	178.80	1.01	1.38	1.16	1.05	1.26	1.18	0.98	1.13
A4	185.00	203.53	1.10	1.77	1.48	1.10	1.46	1.22	1.00	1.30
A5	195.06	225.32	1.16	2.28	1.78	1.15	1.71	1.22	1.00	1.29
Av.			1.08	1.67	1.35	1.10	1.41	1.20	0.99	1.15
St.Dev.			0.06	0.40	0.30	0.04	0.20	0.02	0.01	0.03
C2	168.79	177.18	1.05	1.54	1.30	1.13	1.37	1.39	1.14	1.23
C3	185.51	195.04	1.05	1.82	1.51	1.11	1.49	1.43	1.16	1.32
C4	199.47	220.04	1.10	2.49	1.88	1.17	1.81	1.47	1.19	1.26
C5	235.04	247.78	1.06	2.89	1.94	1.10	1.91	1.35	1.10	1.07
Av.			1.07	2.18	1.66	1.13	1.64	1.41	1.15	1.22
St.Dev.			0.02	0.53	0.27	0.03	0.22	0.04	0.03	0.09

#### 4.4.4 Evaluation of confinement models

There are several confinement models to predict the ultimate strength of the FRP-wrapped concrete columns. In this study, the selected four confinement models that are commonly used by the researchers to predict the ultimate strength of FRP-wrapped low and normal strength concrete columns are also evaluated. These confinement models are presented in Table 6.

As seen in Fig. 9, comparing with the unconfined counterparts, the biggest gain in average

ultimate strength obtained from the our test results for the FRP-wrapped UHPC columns is 16.8% for the specimens G5 (5 layers of GFRP); 22.7% for the specimens A5 (5 layers of AFRP), and 48% for the specimens C5 (5 layers of CFRP), respectively. The increase in ultimate strength for FRP-wrapped columns with different range of concrete compressive strength is also examined by (Shahawy *et al.* 2000, Shehata *et al.* 2002, Ponmalar 2012). A total of 45 CFRP-wrapped concrete columns are tested by Shahawy *et al.* (2000). The average compressive strength of concrete used in the tests is 19 and 49 MPa. When comparing the unconfined counterparts, the average increase in ultimate strength of the CFRP-wrapped columns with concrete compressive strength of 19 MPa and 49 MPa is 74%, 139%, 223%, 290%, and 21%, 56%, 102%, and 130% for the 1, 2, 3, and 4 layers of CFRP sheets, respectively. Totally 12 circular 1 and 2 layers of CFRP-wrapped columns with average compressive strength of concrete varies between 25 and 30 MPa are tested by (Shehata *et al.* 2002). The average increase in ultimate strength is 81% and 138% for columns wrapped with 1 and 2 layers of CFRP sheets, respectively. Similarly, the increase in ultimate strength of GFRP-wrapped columns with average compressive strength of 25 MPa is examined by (Ponmalar 2012). The results show that the increase in ultimate strength is 67%, 129%, and 150% for 1, 2, and 3 layers of GFRP-wrapped concrete columns, respectively. The increase in ultimate strength for FRP-wrapped for low, normal and ultra-high strength concrete columns is shown in Fig. 9.

As clearly seen in Fig. 10, the predictions of these confinement models are too higher than those with our experimental results. This is due to the fact that the increase in ultimate strength for FRP-wrapped UHPC columns is significantly smaller than those with FRP-wrapped low and normal strength concrete columns. In addition, especially, this is more pronounced for the FRP-wrapped UHPC columns with higher confinement ratios than those with smaller confinement ratio. Thus, these confinement models are not convenient and reliable to predict the ultimate strength of the FRP-wrapped UHPC columns. Moreover, a proper confinement model is needed to be developed to better represent the axial behavior of FRP-wrapped UHPC columns by using a large number of test data. However, as seen from Table 5 and Fig. 10, compared with the other confinement models, the model proposed by Samaan *et al.* (1997) can be regarded as more reasonable than the other three confinement models to predict the ultimate strength of the FRP-wrapped UHPC columns. The biggest difference of the ultimate strength between the experimental results and the model proposed by Samaan *et al.* (1997) is 24%. On the other hand, the predictions of the confinement model proposed by Fardis and Khalili (1982) and by Saafi (1999) are very unsafe to predict the ultimate strength of the FRP-wrapped UHPC columns. The biggest difference of the ultimate strength between the experimental results and the model proposed by Saafi (1999) is 91%.

## 6. Conclusions

The main purpose of this study is to predict the axial stress-strain curves and ultimate strengths of the different types of FRP-wrapped UHPC columns. For this purpose, a three dimensional FE model is established and verified by comparison with experimental results. The four damage parameters that are required for CDPM in Abaqus is determined and presented in Table 4 to better represent the axial behavior of FRP-wrapped UHPC columns. A good agreement is achieved between the experimental results and the FE model. The bilinear curve of the FRP-wrapped UHPC columns is successfully obtained. The values of ultimate strength predicted by the FE model show

well enough agreement with the experimental results. However, the FE model provides closer results for the FRP-wrapped UHPC columns with smaller confinement ratio (2, 3 layers of FRP sheets) than those with greater confinement ratio (4, 5 layers of FRP sheets). The biggest difference of ultimate strength between the FE model and the experimental results is 16%.

The reliability of three design codes that is commonly used in America and Canada is evaluated for predicting the ultimate strength of the FRP-wrapped UHPC columns. When comparing with three design codes, the CSA design code requires a minimum confining pressure by applying a reduction coefficient of 0.85 to the unconfined concrete. Thus, the contribution of the confinement effect exerted by the FRP sheets to the concrete core is significantly reduced. As a result of this, the predictions of the CSA design code are more conservative and more reliable than the ACI-440 and the ISIS CANADA design codes. Although the ACI-440 design code are independent of the FRP tensile strength and, especially, are based on limiting the FRP strain, the most unsafe predictions is obtained from this design code. The largest difference of confined concrete strength between the experimental results and the ACI-440 is 47%.

In addition to these findings, the applicability of the selected confinement models that is developed for low and normal strength concrete columns are also investigated for the FRP-wrapped UHPC columns. As seen in Fig. 9, the increase in ultimate strength for the FRP-wrapped UHPC columns is not as significant as for the FRP-wrapped low and normal strength concrete columns. When comparing normal and ultra high strength concrete columns, this increase is more pronounced for the FRP-wrapped low strength concrete columns. Thus, these confinement models are not safely used to predict the ultimate strength of the FRP-wrapped UHPC columns. Furthermore, there is an urgent need to propose a new confinement model for the FRP-wrapped UHPC columns by using a large number of test data. However, when comparing the four selected confinement models, it seems that the predictions of the model proposed by Samaan *et al.* (1997) is more conservative and more reliable than the other design codes for the FRP-wrapped UHPC columns. The biggest difference of the ultimate strength between the experimental results and the confinement model proposed by Samaan *et al.* (1997) is 24%.

## References

- Abaqus (2008), Abaqus version 6.8-1 Manual.
- ACI-440 Committee (2002), "Guide for the design and construction of externally bonded FRP systems for strengthening concrete structures", *ACI 440*, Detroit.
- Al-Salloum, Y.A. (2007), "Influence of edge sharpness on the strength of square concrete columns confined with FRP composite laminates", *Compos. Part B*, **38**(5-6), 640-650
- Canadian Standard Association (CSA) (2002), "Design and construction of building components with fibre-reinforced polymers", *CSA-S806-02*, CSA Rexdale BD, Toronto.
- Cozmanciuc, C., Oltean, R. and Munteanu, V. (2009), "Strengthening Techniques of RC Columns Using Fibre Reinforced Polymeric Materials", *Bul. Inst. Poliytehnice, Iasi, s. Constr., Archit.*, **3**, 85-92.
- Doran, B., Koksal, H.O. and Turgay, T. (2009), "Nonlinear finite element modeling of rectangular/square concrete columns confined with FRP", *Mater. Des.*, **30**(8), 3066-3075.
- Drucker, D.C. and Prager, W. (1952), "Soil mechanics and plastic analysis for limit design", *Q. Appl. Math.*, **10**, 157-165.
- Fardis, M.N. and Khalili, H.H. (1982), "FRP-encased concrete as a structural material", *Mag. Concrete Res.*, **34**(212), 191-202.
- Harmon, T.G. and Slattery, K.T. (1992), "Advanced composite confinement of concrete", *Proceeding of the*

- 1st Int. Conf. on Advanced Composite Materials in Bridges and Structures*, The Canadian Society for Civil Engineering, Montreal, QC, Canada, 299-306.
- Hu, B. and Wang, J.G. (2009), "Comparison of strength, ultimate strain models of concrete columns confined with FRP", *J. Civil Archit. Environ. Eng.*, **31**(5), 9-15.
- Intelligent Sensing for Innovative Structures (ISIS) (2001). "Externally bonded FRP for strengthening reinforced concrete structures." *The Canadian Network of Centres of Excellence on ISIS, ISIS M04*, Winnipeg, Manitoba, Canada.
- Lam, L. and Teng, J.G. (2003), "Design-oriented stress-strain model for FRP-confined concrete in rectangular columns", *J. Reinf. Plast Compos.*, **22**(13), 1149-1186.
- Lee, J. and Fenves, G.L. (1998), "A plastic-damage model for cyclic loading of concrete structures", *J. Eng. Mech.*, **124**, 892-900.
- Lubliner, J., Oliver, J., Oller, S. and Onate, E. (1989), "A plastic-damage model for concrete", *Int. J. Solid Struct.*, **25**, 299-326.
- Mandal, S., Hoskin, A. and Fam, A. (2005), "Influence of concrete strength on confinement effectiveness of fiber-reinforced polymer circular jackets", *ACI Struct. J.*, **102**(3), 383-392.
- Mirmiran, A., Zagers, K. and Wenqing, Y. (2000), "Nonlinear finite element modeling of concrete confined by fiber composites", *Finite elem. Anal. Des.*, **35**(1), 79-96.
- Ponmolar, V. (2012), "Strength comparison of fiber reinforced polymer wrapped concrete exposed to high temperature", *Int. J. Appl. Sci. Eng. Res.*, **1**(2), 146-151.
- Rochette, P. and Labossière, P. (2000), "Axial testing of rectangular column models confined with composites", *ASCE J. Compos. Constr.*, **4**(3), 129-136.
- Saafi, M., Toutanji, H.A. and Li, Z. (1999), "Behavior of concrete columns confined with fiber reinforced polymer tubes", *ACI Mater. J.*, **96**(4), 500-509.
- Shehata, I.A.E.M., Carnerio, L.A.V., and Shehata, L.D.D. (2002), "Strength of short concrete columns confined with CFRP sheets", *Mater. Struct.*, **35**, 50-58.
- Shahawy, M., Mirmiran, A. and Beitelman, B. (2000), "Tests and modeling of carbon-wrapped concrete columns", *Compos.: Part B*, **31**, 471-480.
- Samaan, M., Mirmiran, A. and Shahawy, M. (1997), "Model of concrete confined by fiber composites", *J. Struct. Eng.*, **124**(9), 1025-1031.
- Spoelstra, M.R. and Monti, G. (1999), "FRP-confined concrete model", *J. Compos. Constr.*, **3**(3), 143-150.
- Wang, L.M. and Wu, Y.F. (2008), "Effect of corner radius on the performance of CFRP-confined square concrete columns: Test", *Eng. Struct.*, **30**(2), 493-505.
- Waghmare, S.P.B. (2011), "Materials and jacketing technique for retrofitting of structures", *Int. J. Adv. Eng. Res.*, **1**(1), 15-19.
- Zohrevand, P. and Mirmiran, A. (2011), "Behavior of ultrahigh-performance concrete confined by fiber-reinforced polymers", *J. Mater. Civil Eng.*, **23**(12), 1727-1734.